Citation: Journal of Applied Physics, vol: 109, 083525, pp. null - 2219 (2011)

https://doi.org/10.1063/1.3556451

Transmittance and optical constants of Ho films in the 3-1,340 eV spectral range

Mónica Fernández-Perea[1,2], Juan I. Larruquert[1,*], José A. Aznárez[1], José A. Méndez[1], Luca Poletto[3], Fabio Frassetto[3], A. Marco Malvezzi[4], Daniele Bajoni[4], Angelo Giglia[5], Nicola Mahne[5], Stefano Nannarone[5,6]

[1]GOLD-Instituto de Óptica-Consejo Superior de Investigaciones Científicas

Serrano 144, 28006 Madrid, Spain

[2]Currently at Lawrence Livermore National Laboratory, 7000 East Avenue, Livermore, California 94550, USA

[3]Institute of Photonics and Nanotechnologies-National Council for Research,

via Trasea 7, 35131 Padova, Italy

[4]Dipartimento di Elettronica, Università di Pavia and CNISM, Via Ferrata, 1, I27100 Pavia, Italy

[5]Istituto Officina dei Materiali IOM-CNR Laboratorio TASC, Area Science Park Basovizza, S.S. 14 Km 163.5, 34149 Trieste, Italy

[6]Dipartimento di Ingegneria dei Materiali e dell Ambiente, Universita di Modena e Reggio Emilia, Via Vignolese 905, I-41100 Modena, Italy

ABSTRACT

The optical constants *n* and *k* of holmium (Ho) films were obtained in the 3-1,340-eV range from transmittance measurements performed at room temperature. Thin films of Ho with various thicknesses were deposited by evaporation in ultra high vacuum conditions and their transmittance was measured in situ. Ho films were deposited onto thin C-film substrates supported on high transmittance grids. Transmittance measurements were used to obtain the extinction coefficient *k* of

* Author to whom correspondence should be addressed. Electronic mail: larruquert@io.cfmac.csic.es; fax number: 34 914117651

Ho films. The refractive index *n* of Ho was calculated with Kramers-Krönig analysis; in order to do this, *k* data were extrapolated both on the high and on the low energy parts of the spectrum by using experimental and calculated *k* values available in the literature. Ho, similar to other lanthanides, has a low-absorption band below the $O_{2,3}$ edge onset; the lowest absorption was measured at ~22 eV. Therefore, Ho is a promising material for filters and multilayer coatings in the energy range below the $O_{2,3}$ edge in which most materials have a large absorption. Good consistency of the data resulted from the application of *f* and inertial sum rules.

Keywords: Extreme Ultraviolet; Far Ultraviolet; Optical constants; Holmium; Absorption filters; Multilayers; Optical properties of thin films

1. Introduction

Until recently, lanthanides had not been fully characterized in the extreme ultraviolet (EUV)-soft X-rays. However, an increased interest has grown on these materials with the recent characterization of Yb[1,2], La[3,4], Tb[3,4], Gd[5,4], Nd[5,4], Ce[6], Pr[7], Eu[8], Dy[4], Tm[9], and Lu[10], and of materials with close chemical properties such as Sc[11,12,13,14] and Y[15]. This paper addresses the optical properties of Ho films in the 3-1,340-eV range. The optical properties in this energy range are characterized by the high energy tail of the valence electrons and by the presence of two intense $O_{2,3,}$ and $N_{4.5}$ absorption bands, in order of increasing binding energy, due to the excitation of 5p, and 4d electrons, respectively, above the Fermi level.

Scarce data are available on the optical properties of Ho in the UV to soft X-rays. Gribovskii and Zimkina[16] determined the mass absorption coefficient of most rare-earth elements in the 70-500-eV range, which encloses Ho $N_{4,5}$ edge. Vicentin et al.[17] performed transmittance measurements on Ho films and other lanthanides and obtained the absorption coefficient at the $M_{4,5}$ edge. Ott et al.[18] measured the optical constants of a Ho film at the $M_{4,5}$ edge through reflectance measurements performed at 40 K. Zimkina et al.[19] and Fomichev et al.[20] performed absorption measurements and provided data of the product of the absorption coefficient times the film thickness in the 60-460 eV and 161-180 eV ranges, respectively; however, these papers cannot be directly taken for absolute reference since the absorption coefficient cannot be deduced. Pétrakian[21] measured the absorption of thin films of Ho in the 1.5-6 eV range and provided data of the product of the absorption coefficient times the film thickness. Sugar[22] calculated the relative positions of the $4d^{10}4f^{14}4I_{15/2}$ to $4d^{9}4f^{12}$ transitions and compared them with the peaks close to $N_{4,5}$ reported in Ref. 19. Fischer and Baun[23] obtained absorption spectra of lanthanides and lanthanide oxides at the $M_{4,5}$ edges; they only plotted the data for the oxides but they stated that the spectrum did not show any difference between metal

and oxide; however, no absorption scale was plotted. Thole et al.[24] plotted absorption of lanthanide samples including Ho with focus on a small energy range in the region of the M_5 edge aiming at line shape analysis to determine the multiplet components contributing to the absorption peak; since the preparation of the samples is not clearly described and the ordinates in the plotted figures are not clear, the data can only be used qualitatively for the position of the absorption peaks. Tracy[25] obtained spectra of vapors of Ho and other lanthanides in the ~21-40 eV range, and reported relative absorption cross-section plots. Padalia et al.[26] obtained absorption spectra of Ho and other lanthanides at $L_{2,3}$ edges. Materlik et al.[27] measured L-edge absorption spectra of Ho and other lanthanides. In the low-energy range covered here and at lower energies, Weaver and Lynch[28] measured the absorptivity of oriented single crystals of Ho and other lanthanides in the 0.2-4.4-eV range at 4.2 K; starting with these data, the complex dielectric constant and the optical constants *n*, *k* in the 0.1-5 eV range were reported in two crystallographic directions[29]. Krizek and Taylor[30] provided data of the optical conductivity and ε_1 of Ho and other lanthanides obtained from ellipsometry measurements in the 0.35-2.5 eV range at and below room temperature. Krizek et al.[31] reported Drude parameters for polycrystalline films of Ho and other lanthanides. Weber[32] reported infrared data on reflectivity and conductivity of single crystals and of thin films of Ho at various temperatures.

Other than optical measurements, Bakulin et al.[33] measured the characteristic energy losses of electrons for samples of Ho and other lanthanides; they determined the excitation energies of the plasma oscillations and the interband excitations. Trebbia and Colliex[34] performed electron-energy-loss spectroscopy on films of Ho and other lanthanides and they reported the oscillator strength close to the $N_{4,5}$ edge. Colliex et al.[35] measured the energy loss spectra of electrons transmitted through thin films of Ho and other rare-earth metals and their compounds and reported the energies of the plasmon peaks. Borovskii and Komarov[36] obtained the absorption coefficient of Ho and other

lanthanides from electron-energy-loss spectra; the data covered the $N_{4,5}$ range but were reported without units. Strasser et al.[37] reported reflection electron-energy-loss spectra of films of Ho and other lanthanides in the region around $N_{4,5}$ edge. Della Valle and Modesti[38] reported reflection electron-energy-loss spectra of Ho and other lanthanides. Bonnelle *et al.*[39] reported photoelectron spectra of Ho_2O_3 in the valence region and the 4d region. Kaindl et al.[40] obtained the x-ray absorption through measurements of total electron yield of many compounds including Ho_2O_3 at $M_{4,5}$ edge. Sugar et al.[41] performed x-ray photoabsorption spectra of HoF_3 and other lanthanide fluorides at $M_{4,5}$ edge from measurements of total electron yield. Dzionk et al.[42] measured the photoion yield spectra generated by EUV radiation on atomic beams of Ho and other lanthanides. Electron-energy-loss spectroscopy in reflection mode of Ho and other lanthanides was investigated by Netzer et al.[43]. Henke et al.[44] obtained a semi-empirical set of data in the 30-10,000-eV range (later extended to 30,000 eV[45]). Nagao and Igarashi[46] calculated the absorption coefficient of Ho at the M_4 and M_5 edges and reported them in arbitrary units. In addition to the above references, Weaver et al.[29] reviewed published data on the optical constants of Ho and other lanthanides.

This paper is aimed at providing accurate data on pure Ho samples in a broad spectral range in view of the scarce and disperse data in the literature. It is organized as follows. A brief description of the experimental techniques used in this research is given in Section 2. Section 3 presents transmittance data, extinction coefficient of Ho calculated from transmittance, and dispersion obtained using Kramers-Krönig (KK) analysis; the consistency of the data gathered in this research is also evaluated.

2. Experimental techniques

2.1 SAMPLE PREPARATION

Both Ho film deposition and characterization were performed under ultra high vacuum (UHV) at BEAR beamline of ELETTRA synchrotron (Trieste, Italy)[47]. Ho films were deposited onto 5-nm thick C films supported on 117 mesh Ni grids with 88.6% nominal open area (pitch of 216 μm). The procedure for C film preparation was reported elsewhere[13]. Ho films were deposited with a TriCon evaporation source[48], in which a small Ta crucible is bombarded by electrons that impinge on the crucible wall. Ho granules of 99.98 % purity from LTS Chem. Inc. were used. The crucible-sample distance was 200 mm. Deposition rate was ~4 nm/min. Chamber pressure during deposition was ~2×10^{-7} Pa. Ho films were deposited onto room-temperature substrates. Film thickness was monitored with a quartz crystal microbalance during deposition. A witness glass substrate was placed close to the grid-supported C film to get coated simultaneously with a similar Ho film thickness. The distance on samples between the area of transmittance measurements and that of reflectance measurements was less than 10 mm. Reflectance versus the incidence angle was measured on the witness samples at the energy of 98 eV and the angular positions of the minima and maxima were used to calculate the Ho film thickness. Since reflectance measurements were performed far from absorption edges, Henke optical constants[45] could be used in this calculation. Henke data were downloaded from the website of the Center for X-Ray Optics (CXRO) at Lawrence Berkeley National Laboratory[49].

2.2 EXPERIMENTAL SETUP FOR TRANSMITTANCE MEASUREMENTS

Transmittance measurements were performed at BEAR beamline with a vertical exit slit of 100 μm (above 24 eV) and 450 μm (below 24 eV); the monochromator spectral resolution E/ΔE varied between 500 and 2000, depending on slit widths. The suppression of higher orders was achieved using quartz, LiF, In, Sn, Al, and Si filters at specific ranges below ~100 eV, and choosing a plane

mirror-to-grating deviation angle in the monochromator setup that minimized the higher-order contribution at energies above 100 eV. The beam cross section at the sample was about 0.7×1.5 mm^2 FWHM.

The measurements were performed in the BEAR spectroscopy chamber[50]; a gate valve separates this chamber from the preparation chamber, where samples were prepared in situ. Two C substrates were used and their transmittance was measured previously to Ho deposition. Three and two successive Ho coatings of various thicknesses were accumulated upon the first and the second substrate, respectively, without breaking vacuum. Each sample was transferred back and forth between the deposition chamber and the measurement chamber, always under UHV, for the deposition of the successive Ho layers and their characterization. Transmittance measurements were performed onto samples at room temperature. For each film, uniformity evaluations were performed. We estimate that the overall uncertainty in the transmittance measurements is of the order of 2%. At energies above 18 eV, fluctuations of the photon beam during transmittance measurements were recorded with a 100-V biased, Au mesh. These fluctuations were cancelled by normalizing the recorded beam intensity to the mesh current. At energies below 18 eV, fluctuations were cancelled by normalization with respect to the ring current.

3. Results and discussion

3.1 TRANSMITTANCE AND EXTINCTION COEFFICIENT OF Ho

We measured the transmittance of Ho films with the following thicknesses: 19.1, 28.7, 39.5, 64.7, and 125.9 nm. The transmittance of the Ho films normalized to the transmittance of the uncoated substrate is plotted in Fig. 1. There are three high-transmission bands peaked at ~1,330 (on the edge of our measurements), ~156.5, and ~21.5-22 eV, right below Ho M_5, $N_{4,5,}$ and $O_{2,3}$ edges, respectively. The low-energy band of relatively large transmittance extends within ~17-23-eV. Close

large-transmittance bands have been measured for other rare earths; hence Ho, as other lanthanides such as La, Ce, Pr, Nd, Eu, Gd, Tb, Dy, Tm, Yb, and Lu, is a promising material for transmittance filters or multilayer spacers for the extreme ultraviolet in the ~17-23-eV spectral range, where there has been a lack of low-absorbing materials until recently. A small oscillation at ~315 eV can be attributed to Ho N_3 edge. The slight oscillations at ~100, ~285, ~405, ~460, and ~537 eV are related to data normalization, due to the fact that at these energies there is an abrupt decrease of the signal due to the presence of the Si filter, to carbon contamination of the optics, and to the slight presence of N, Ti, and O either at the optics, at the detector, or on the sample.

If the contribution to transmittance coming from multiple reflections inside the Ho film is negligible, the extinction coefficient *k* (the imaginary part of the complex refractive index) can be calculated from transmittance with the following equation:

$$\ln\left(\frac{T_{fs}}{T_s}\right) \approx A - \left(\frac{4\pi k}{\lambda}\right) \cdot d \qquad (1)$$

where T_s and T_{fs} represent the transmittance of the uncoated substrate and of the substrate coated with a Ho film, respectively; λ is the radiation wavelength in vacuum; *d* stands for the Ho film thickness. Eq. (1) is a straightforward derivation of the well-known Beer-Lambert law. A is a constant for each energy and encompasses the terms that involve reflectance, in the assumption that multiple reflections are negligible.

k of Ho films was calculated by fitting the slope of the logarithm of transmittance versus thickness at each energy using Eq. (1). Examples of transmittance measurements versus the film thickness for five photon energies are given in Fig. 2, along with their fittings. *k* data so obtained are represented in Fig. 3 versus the photon energy. The semi-empirical data of Henke[45,49] are also plotted in Fig. 3. The aforementioned presence of Si, C, Ti, N, and O oscillations at the Si $L_{2,3}$, C K, Ti $L_{2,3}$, N K, and

O K edges on transmittance has weakened or disappeared on *k* because measurements on samples of different Ho thicknesses with similar presence of contaminants (either on the sample, on the detector or on the light path), or with artifacts coming from normalization at transmittance calculation, will tend to cancel out in the calculation of *k* with the slope method.

The density of Ho films is needed to calculate Henke data. We measured it because the density of thin films may be somewhat lower than the reported data for the bulk material. To do this we deposited a thin film of Ho onto an Al foil. We weighed the Al foil both before and after the Ho deposition with a precision of $\pm 1\times10^{-5}$ g. The thickness of the Ho film was measured by Tolansky interferometry on a witness sample. We measured the surface area of the deposit with an optical comparator. We obtained a density of 8.33±0.25 g/cm^3 for the Ho film. Several tabulated values for bulk Ho were found, most of them close to 8.80 g/cm^3. Hence, the measured density of the film is slightly smaller than that of bulk Ho. The density value measured for the thin film was used to calculate Henke data.

When reflectance is not negligible, the application of Eq. (1) to calculate *k* through the slope of the log of transmittance versus thickness may result in uncertainties. In order to overcome this, we proceeded in an iterative way. For the first iteration, initial *k* values were obtained using the slope method. These values, along with *k* data in the rest of the spectrum, were used to obtain the refractive index *n* (the real part of the complex refractive index) with KK analysis (KK analysis is described in sub-section 3.2). Once a first set of data {$n(E)$, $k(E)$} was available, the transmittance ratio of the C/Ho bilayer to the single C film was calculated with the usual equations based on Fresnel coefficients. This transmittance ratio was compared with the measured data; the difference between measured and calculated transmittance gave us an estimate to modify *k*. This modified value was a second estimate of *k*, from which a second estimate of *n* was obtained with KK analysis. This

procedure can be iterated until the best match to transmittance data is obtained. The optical constants of the single C film at this same range had been previously calculated with a similar procedure starting with *k* obtained from the transmittance of an uncoated C substrate. The iterative method was applied in the 3-40-eV range. The *k* data plotted in Fig. 3 were somewhat modified at 3 eV in an attempt to better match literature data.

In the calculation of *k* in the range below ~100 eV, transmittance data of the two thickest films was found to be somewhat deviated from the data coming from the 3 thinnest films. Furthermore, *k* data calculated with all samples was found to deviate with respect to Henke data in the range between $O_{2,3}$ edge and ~100 eV. Therefore, in the calculation of *k* we decided to use only the three thinnest films below 100 eV, whereas all 5 films were used at $N_{4,5}$ edge and above, with a smooth connection in between; this resulted in a better match with Henke data below 100 eV.

k values at the $O_{2,3}$ edge and around are presented in Fig. 4. The smallest value of *k* is obtained at ~22.0 eV. This minimum is close to the ones obtained for other rare earths: Ce[6] at 16.1 eV, La[3] at 16.5 eV, Eu[8] at 16.7 eV, Pr[7] at 16.87 eV, Nd[5] at ~ 17 eV, Tb[3] at ~19.5 eV, Gd[5] at ~19.7 eV, Dy[4] at ~20.2 eV, Yb[1,2] at 21.2 eV, Tm[9] at 23 eV, Lu[10] at 25.1 eV, and Sc[11] (neighbor in the periodic table) at 27 eV. As with other lanthanides, optical properties of Ho in this range are promising for its use in transmittance filters or reflective multilayers. However, Ho, as the other lanthanides, is a reactive material, and this may result in the need to develop a protective layer.

Fig. 5 displays *k* around Ho $N_{4,5}$ edge, along with experimental data of Gribovskii and Zimkina[16] and semi-empirical data of Henke et al. The current data show a structure of three narrow peaks at 157.75, 158.88, 160.88 eV, and two broader and higher peaks at 166.3, 171.0 eV. The peaks are related to transitions from 4d to 4f shells. Zimkina et al.[19] reported three peaks at 155.8, 156.9, and

158.8 eV, and their data does not reach the energy range of our broader peaks. Sugar[22] calculated the position of the peaks. In addition to the peaks measured by Zimkina et al., Sugar obtained 9 peaks between 161.7 and 174.6 eV that he related to a single experimental peak observed by Zimkina et al.[19] at ~167 eV. The latter can be associated with our two broader peaks. Gribovskii's data match well our data, but the former data have a much coarser sampling. Hence, regardless of the precision of the exact peak energies, we provide here first quantitative *k* data at both narrow and broad peaks at the $N_{4,5}$ range.

At ~1,000 eV (see Fig. 1), two transmittance-versus-energy curves intersect for reasons that are not well understood. In the calculation of *k* at these high energies we decided to use the measurements on all samples since we had no guide to reject any data.

3.2 REFRACTIVE INDEX CALCULATION THROUGH DISPERSION RELATIONS

The refractive index *n* of Ho was calculated using KK dispersion relations:

$$n(E)-1=\frac{2}{\pi}P\int_0^{\infty}\frac{E'k(E')}{E'^2-E^2}dE' \qquad (2)$$

where *P* stands for the Cauchy principal value. The application of Eq. (2) to calculate *n* requires the availability of *k* data over the whole spectrum, so that we extended the present data with the available data in the literature and extrapolations.

At the Ho $M_{4,5}$ edge we could use the data of Vicentin et al.[17] and Ott et al.[18]. *k* data at the $M_{4,5}$ edge can be immediately obtained from the absorption coefficient reported by Vicentin et al.[17]. Ott et al.[18] reported both optical constants at the M_5 edge. However, Vicentin's M_5 peak was about twice the value of that of Ott et al. In principle, the data published by Vicentin et al. were obtained in excellent conditions to result in precise data. Since Vicentin's paper reported data not only of Ho but also Gd,

Dy, and Er, we could compare their experimental results to literature data. In a separate paper devoted to Er optical constants[51], we obtained that Vicentin's *k* value at Er M_5 edge was much larger than our data. Furthermore, Vicentin's *k* data at Gd M_5 edge was 0.0114, whereas we derived, using the transmittance data reported in the Fig. 2 of the paper of Peters et al.[52], a value of 0.0074 at this same Gd M_5 edge. Hence we suspect that all Vicentin's data may be somewhat too large. Furthermore, we represented $M_{4,5}$-edge *k* data of several lanthanides that we have been gathering in this long-run research and we found that Vicentin's data for Ho was far above the trend of lanthanides; even Ott's data was somewhat larger than this trend. All the above convinced us not to use Vicentin's data directly, although we did it indirectly in the following way. We could have used Ott's data, but they did not report on the M_4 edge. Then we merged the two data sets: we used Vicentin's data but we scaled both their M_4 and M_5 peaks down in a factor given by the Ott-to-Vicentin's M_5 peak *k* data ratio. Above the M_4 edge we smoothly connected these data with those of Henke. Fig. 6 displays the data so constructed, which is referred to as *rescaled Vicentin*, along with the experimental data of Vicentin et al.[17], Ott et al.[18], and the semi-empirical data of Henke. The inset compares in logarithmic scale the data of Ott et al. [18] with the original data of Vicentin et al.[17].

Further extrapolations were as follows. Between 1,400 and $3 \cdot 10^4$ eV we used Henke data from CXRO's web[45,49]. For even larger energies, the calculations of Chantler et al.[53] were used up to $4.3 \cdot 10^5$ eV. The extrapolation to infinity was performed by keeping constant the slope of the log-log plot of $k(E)$ of Chantler's data. At energies smaller than the present ones, we used the data of Krizek and Taylor[30], from whose conductivity and ε_1 data we could immediately obtain *k* in the 0.38-2.6 eV range. This was preferred over using the data of Weaver and Lynch[28] because the latter was measured on single crystals, compared to our films, and their use would require an average over the two sets of optical constants measured at the two main axes. The extrapolation to zero energy was performed by fitting a Drude model on Krizek's data.

Fig. 7 displays *k* data of Ho obtained in the present research along with literature data, calculations, and extrapolations that were gathered for KK analysis.

Fig. 8 displays δ=1-*n* calculated with Eq. (2) using the data plotted in Fig. 7; *n* and δ at $O_{2,3}$, and $N_{4,5}$ edges are shown in Figs. 9 to 10, respectively. We also plot δ that was calculated at the $M_{4,5}$ edge, which is given in Fig. 11. Ott's data and the semi-empirical data of Henke are also plotted for comparison. δ data obtained at the M_5 edge are relatively close to Ott's data, with a shift in energy of 3.4 eV, which is similar to the energy difference between Vicentin's and Ott's data for M_5 peak *k* data.

3.3 CONSISTENCY OF OPTICAL CONSTANTS

The *f* sum rule relates the number density of electrons to *k* (or to other functions); it provides a guidance to evaluate the global accuracy of *k* data. It is useful to define the effective number of electrons per atom $n_{eff}(E)$ contributing to *k* up to given energy *E*:

$$n_{eff}(E) = \frac{4\varepsilon_0 m}{\pi N_{at} e^2 h^2} \int_0^E E' k(E') dE' \qquad (3)$$

where N_{at} is the atom density, *e* is the electron charge, ε_0 is the permittivity of vacuum, *m* is the electron mass, and *h* is Planck's constant[54]. The *f* sum rule expresses that the high-energy limit of the effective number of electrons must reach Z=67, i.e., the atomic number of Ho. When the relativistic correction on scattering factors is taken into account, the high-energy limit of Eq. (3) is somewhat modified. The following modified Z was adopted here: Z*=65.88[55]. The high-energy limit that we obtained by integrating the data set plotted in Fig. 7 using Eq. (3) was 65.28, which is only 0.9% smaller than the above Z* value. The main contribution to n_{eff} was found to come from the ~1 to 4×10^5 eV range. The small difference with Z^* may come from inaccuracies in the film thickness

determination, in the transmittance measurements, and in the *k* data used in the energy extrapolations.

A useful test to evaluate the accuracy of KK analysis is obtained with the inertial sum rule:

$$\int_0^\infty [n(E)-1]dE = 0 \tag{4}$$

which expresses that the average of the refractive index throughout the spectrum is unity. The following parameter is defined to evaluate how close to zero the integral of Eq. (5)[56] is:

$$\zeta = \frac{\int_0^\infty [n(E)-1]dE}{\int_0^\infty |n(E)-1|dE} \tag{5}$$

Shiles et al.[54] suggested that a good value of ζ should stand within ±0.005. An evaluation parameter ζ=-4×10^{-4} was obtained here with the *n* data calculated in this research. Therefore, the inertial sum rule test is well within the above top value, which, along with the result obtained above for the *f* sum rule, suggest good consistency of *n* and *k* data.

CONCLUSIONS

The transmittance of thin films of Ho deposited by evaporation has been measured in situ in the 3-1,340 eV photon energy range under UHV conditions. The extinction coefficient *k* of Ho has been calculated from transmittance measurements in the same spectral range. Ho features an absorption minimum at 22 eV. This relatively low absorption at this spectral range makes Ho a promising candidate for transmittance filters and reflective multilayers. Given the reactivity of Ho, as with other lanthanides, a surface passivation method is expected to be required to prevent surface instability of Ho in contact with atmosphere.

The refractive index *n* of Ho in the same range was obtained with KK analysis over an extended spectral range.

The current data encompass the extinction coefficient and the refractive index data of Ho at the $N_{4,5}$ and $O_{2,3}$ edges. It is also proposed a rescaling for the data available in the literature at the $M_{4,5}$ edge.

The evaluation of *f* and inertial sum rules shows good consistency of the optical constants of Ho.

ACKNOWLEDGMENTS

We acknowledge support by the European Community - Research Infrastructure Action under the FP6 "Structuring the European Research Area" Programme (through the Integrated Infrastructure Initiative "Integrating Activity on Synchrotron and Free Electron Laser Science"). This work was also supported by the National Programme for Space Research, Subdirección General de Proyectos de Investigación, Ministerio de Ciencia y Tecnología, project numbers AYA2008-06423-C03-02/ESP, AYA2009-14070, and AYA2010-22032. A. M. M. acknowledges the partial support of the Fondo d'Ateneo per la Ricerca (FAR) of Università di Pavia. The technical assistance of J. M. Sánchez-Orejuela is acknowledged.

REFERENCES

1. J. I. Larruquert, J. A. Aznárez, J. A. Méndez, José Calvo-Angós, "Optical properties of Yb films in the far and the extreme ultraviolet", Appl. Opt. **42**, 4566-4572 (2003).

2. M. Fernández-Perea, J. I. Larruquert, J. A. Aznárez, J. A. Méndez, L. Poletto, D. Garoli, A. M. Malvezzi, A. Giglia, S. Nannarone "Determination of the transmittance and extinction coefficient of Yb films in the 23-1,700-eV range", J. Opt. Soc. Am. A **24**, 3691-3699 (2007).

3. Yu. Uspenski, J. Seely, N. Popov, I. Artioukov, A. Vinogradov, D. Windt, B. Kjornrattanawanich, "Extreme UV optical constants of rare-earth metals free from effects of air contamination", in *Soft X-Ray Lasers and Applications VI*, E. E. Fill, ed., Proc. SPIE **5919**, 213-220 (2005).

4. B. Kjornrattanawanich, D. L. Windt, J. A. Bellotti, J. F.Seely, "Measurement of dysprosium optical constants in the 2–830 eV spectral range using a transmittance method, and compilation of the revised optical constants of lanthanum, terbium, neodymium, and gadolinium", Appl. Opt. **48**, 3084-3093 (2009).

5. B. Kjornrattanawanich, D. L. Windt, Y. A. Uspenskii, J. F. Seely, "Optical constants determination of neodymium and gadolinium in the 3 nm to 100 nm wavelength range", in *Advances in X-ray/EUV optics, components, and applications*, A. M. Khounsary, C. Morawe, eds., Proc. of SPIE **6317**, 63170U (2006).

6. M. Fernández-Perea, J. I. Larruquert, J. A. Aznárez, J. A. Méndez, L. Poletto, D. Garoli, A. M. Malvezzi, A. Giglia, S. Nannarone "Determination of the transmittance and extinction coefficient of Ce films in the 6-1,200-eV range", J. Appl. Phys. **103**, 073501-1 to -7 (2008).

7. M. Fernández-Perea M. Vidal-Dasilva, , J. A. Aznárez, J. I. Larruquert, J. A. Méndez, L. Poletto, D. Garoli, A. M. Malvezzi, A. Giglia, S. Nannarone "Determination of the transmittance and extinction coefficient of Pr films in the 4-1,600-eV range", J. Appl. Phys. **103**, 113515-1 a -7 (2008).

8. M. Fernández-Perea M. Vidal-Dasilva, J. A. Aznárez, J. I. Larruquert, J. A. Méndez, L. Poletto, D. Garoli, A. M. Malvezzi, A. Giglia, S. Nannarone "Determination of the transmittance and extinction coefficient of Eu films in the 8.3-1,400-eV range", J. Appl. Phys. **104**, 123527-1 a -7 (2008).

9. Manuela Vidal-Dasilva, Mónica Fernández-Perea, José A. Aznárez, Juan I. Larruquert, José A. Méndez, Luca Poletto, A. Marco Malvezzi, Angelo Giglia, Stefano Nannarone, "Transmittance and optical constants of Tm films in the 2.75-1,600 eV spectral range", J. Appl. Phys. **105**, 103110 (2009).

10. S. García-Cortés, L. Rodríguez-de Marcos, J. I. Larruquert, J. A. Aznárez, J. A. Méndez, L. Poletto, F. Frassetto, A. M. Malvezzi, A. Giglia, N. Mahne, S. Nannarone, "Transmittance and optical constants of Lu films in the 3-1800 eV spectral range", J. Appl. Phys. **108**, 063514 (2010).

11. A. L. Aquila, F. Salmassi, E. M. Gullikson, F. Eriksson, J. Birch, "Measurements of the optical constants of scandium in the 50-1300 eV range", in *Optical constants of materials for UV to x-ray wavelengths*, R. Soufli and J. F. Seely, eds., Proc. of SPIE **5538**, 64-71 (2004).

12. Y. A. Uspenskii, J. F. Seely, N. L. Popov, A. V. Vinogradov, Y. P. Pershin, and V. V. Kondratenko, "Efficient method for the determination of extreme-ultraviolet optical constants in reactive materials: application to scandium and titanium", J. Opt. Soc. Am. A **21**, 298-305 (2004).

13. J. I. Larruquert, J. A. Aznárez, J. A. Méndez, A. M. Malvezzi, L. Poletto, S. Covini, "Optical properties of Sc films in the far and the extreme ultraviolet", Appl. Opt. **43**, 3271-3278 (2004).

14. M. Fernández-Perea, J. I. Larruquert, J. A. Aznárez, J. A. Méndez, L. Poletto, A. M. Malvezzi, A. Giglia, S. Nannarone, "Determination of optical constants of scandium films in the 20-1000 eV range", J. Opt. Soc. Am. A 23, 2880-2887 (2006)

15. B. Sae-Lao, R. Soufli, "Measurements of the refractive index of Yttrium in the 50-1300 eV energy range", Appl. Opt. **41**, 7309-7316 (2002).

16. S. A. Gribovskii and T. M. Zimkina, "Absorption coefficients of rare earth elements of the lanthanum group in the ultrasoft X-ray region", Opt. Spectrosc. **35**, 104-105 (1973).

17. F. C. Vicentin, S. Turchini, F. Yubero, J. Vogel, M. Sacchi, "Absorption cross sections at the M4,5 edges of rare earths: a soft X-ray transmission experiment", J. Electron Spectrosc. Relat. Phenom. **74**, 187-194 (1995).

18. H. Ott, C. Schüßler-Langeheine, E. Schierle, A. Yu. Grigoriev, V. Leiner, H. Zabel, G. Kaindl, and E. Weschke, "Magnetic x-ray scattering at the M5 absorption edge of Ho", Phys. Rev. B **74**, 094412 (2006).

19. T. M. Zimkina, V. A. Fomichev, S. A. Gribovskii, I. I. Zhukova, “Anomalies in the character of the x-ray absorption of rare-earth elements of the lanthanide group”, Sov. Phys.- Sol. State **9**, 1128-1130 (1967).

20. V. A. Fomichev, T. M. Zimkina, S. A. Gribovskii, I. I. Zhukova, “Discrete absorption by 4d electrons in the lanthanum group rare-earth metals”, Sov. Phys.- Sol. State **9**, 1163-1165 (1967).

21. J. P. Pétrakian, “New investigation of the optical absorption of rare-earth thin films”, Thin Solid Films **13**, 269-273 (1972).

22. J. Sugar, “Potential-barrier effects in photoabsorption. II Interpretation of photoabsorption resonances in lanthanide metals at the 4*d*-electron threshold”, Phys. Rev. B **5**, 1785-1792 (1972).

23. D. W. Fischer, W. L. Baun, “Self-absorption effects in the soft x-ray M_α and M_β emission spectra of the rare earth elements”, J. Appl. Phys. 38, 4830-4836 (1967).

24. B. T. Thole, G. van der Laan, and J. C. Fuggle, G. A. Sawatzky, R. C. Karnatak, J.-M. Esteva, “*3d* x-ray-absorption lines and the $3d^9 4f^{n+1}$ multiplets of the lanthanides”, Phys. Rev. B **32**, 5107-5118 (1985).

25. D. H. Tracy, “Photoabsorption structure in lanthanides: 5p subshell spectra of Sm I, Eu I, Dy I, Ho I, Er I, Tm I, and Yb I”, Proc. R. Soc. Lond. A **357**, 485-498 (1977).

26. B. D. Padalia, S. N. Gupta, V. P. Vijayavargiya, B. C. Tripathi, “X ray spectroscopic study of 4f heavy rare earth metals”, J. Phys. F **4**, 938-946 (1974).

27. G. Materlik, J. E. Müller, J. W. Wilkins, “L-edge absorption spectra of the rare earths: assessment of the single-particle picture”, Phys. Rev. Lett. **50**, 267-270 (1983).

28. J. H. Weaver, D. W. Lynch, “Anisotropic optical properties of heavy-rare-earth single crystals”, Phys. Rev. Lett. **34**, 1324-1327 (1975).

29. J. H. Weaver, C. Krafka, D. W. Lynch, and E. E. Koch, “Physics Data. Optical properties of metals”, volume 18-2, Fachinformationszentrum Energie-Physik-Mathematik, GmbH, Karlsruhe, Germany, 1981.

30. J. Krizek, K. N. R. Taylor, “Optical properties of rare-earth films in paramagnetic and magnetically ordered phases”, J. Phys. F. **5**, 774-789 (1975).

31. J. Krizek, K. N. R. Taylor, H. Krizek, “Room temperature optical properties of rare earths”, Phys. Stat. Sol. B 77, 725-730 (1976).

32. P. Weber, “Spin Dependent Transport and Magnetic Ordering in Rare Earth Metals”, Thesis, Univ. Stuttgart (Germany), 2004.

33. E. A. Bakulin, L. A. Balabanova, E. V. Stepin, V. V. Shcherbinina, “Characteristics energy losses of electrons in the rare-earth metals”, Sov. Phys.- Sol. State **13**, 189-191 (1971).

[34]. P. Trebbia, C. Colliex, “Study of the excitation of 4d electrons in rare-earth metals by inelastic scattering of a high energy electrón beam”, Phys. Stat. Sol. (b) **58**, 523-532 (1973).

[35]. C. Colliex, M. Gasgnier, P. Trebbia, “Analysis of the electron excitation spectra in heavy rare earth metals, hydrides and oxides”, J. Physique **37**, 397-406 (1976).

36. I. B. Borovskii, Ya. Komarov, “Structure of the spectra of characteristic energy losses of reflected electrons in Gd, Tb, Dy, and Ho”, Sov. Phys. Dokl. **21**, 735-737 (1976).

37. G. Strasser, G. Rosina, J. A. D. Matthew, F. P. Netzer, “Core level excitations in the lanthanides by electron energy loss spectroscopy. I: 4d and 3d excitations”, J. Phys. F: Met. Phys. **15**, 739-751 (1985).

38. F. Della Valle, S. Modesti, “Exchange-excited *f-f* transitions in the electron-energy-loss spectra of rare-earth metals”, Phys. Rev. B **40**, 933-941 (1989).

39. C. Bonnelle, R. C. Karnatak, C. K. Jørgensen, “X-ray and photoelectron spectroscopy for the determination of 4f energies of rare earths”, Chem. Phys. Lett. **14**, 145-149 (1972).

40. G. Kaindl, G. Kalkowski, W. D. Brewer, B. Perscheid, F. Holtzberg, “M-edge x-ray absorption spectroscopy of 4*f* instabilities in rare-earth systems”, J. Appl. Phys. **55**, 1910-1915 (1984).

41. J. Sugar, W. D. Brewer, G. Kalkowski, G. Kaindl, E. Paparazzo, “Photoabsorption by the 3d shell in Ce, Pr, Ho, and Er: Observations and calculations”, Phys. Rev. A **32**, 2242-2248 (1985).

42. Ch. Dzionk, W. Fiedler, M. v. Lucke, P. Zimmermann, “Photoion yield spectra of the lanthanides in the region of the 5*p* excitation: the elements Gd, Tb, Dy, Ho, Er, Tm, and Yb”, Phys. Rev. A, **41**, 3572-3574 (1990).

43. F. P. Netzer, G. Strasser, G. Rosina, J. A. D. Matthew, “Valence excitations of rare earths by electron energy loss spectroscopy“, Surf. Sci. **152/153**, 757-764 (1985).

44. B.L. Henke, P. Lee, T. J. Tanaka, R. L. Shimabukuro, B. K. Fujikawa, “Low-Energy X-Ray Interaction Coefficients: Photoabsorption, Scattering, and Reflection, E = 100-2000 eV, *Z*=1-94”, At. Data Nucl. Data Tables **27**, 1-144 (1982).

45. B.L. Henke, E.M. Gullikson, and J.C. Davis, “X-ray interactions: photoabsorption, scattering, transmission, and reflection at E=50-30000 eV, Z=1-92”, Atomic Data and Nuclear Data Tables **54**, 181-342 (1993).

46. Tatsuya Nagao and Jun-ichi Igarashi, “Satellite Holmium M-Edge Spectra from the Magnetic Phase via Resonant Soft X-Ray Scattering”, J. Phys. Soc. Japan **77**, 084710 (2008)

47. S. Nannarone, F. Borgatti, A. De Luisa, B. P. Doyle, G. C. Gazzadi, A. Giglia, P. Finetti, N. Mahne, L. Pasquali, M. Pedio, G. Selvaggi, G. Naletto, M. G. Pelizzo, G. Tondello, “The BEAR Beamline at Elettra”, T. Warwick, J. Arthur, H. A. Padmore, J. Stöhr, eds., AIP Conference Proceedings **705**, 450-453 (2004).

48. R. Verucchi, S. Nannarone, “Triode electron bombardment evaporation source for ultrahigh vacuum thin film deposition”, Rev. Sci. Instrum. **71**, 3444-3450 (2000).

49. http://henke.lbl.gov/optical_constants/

50. L. Pasquali, A. De Luisa, S. Nannarone, “The UHV Experimental Chamber For Optical Measurements (Reflectivity and Absorption) and Angle Resolved Photoemission of the BEAR Beamline at ELETTRA”, T. Warwick, J. Arthur, H.A. Padmore, J. Stöhr, eds., *AIP Conference Proceedings* ***705****, 1142-1145 (2004)*

51. J. I. Larruquert, F. Frassetto, S. García-Cortés, M. Vidal-Dasilva, M. Fernández-Pereaa, José A. Aznárez, José A. Méndez, L. Poletto, A. M. Malvezzi, A. Giglia, S. Nannarone, “Transmittance and optical constants of Er films in the 3.25-1,580 eV spectral range”, submitted for publication.

52. J. F. Peters, J. Miguel, M. A. de Vries, O. M. Toulemonde, J. B. Goedkoop, S. S. Dhesi, N. B. Brookes, “Soft x-ray resonant magneto-optical constants at the Gd M4,5 and Fe L2,3 edges”, Phys. Rev. B **70**, 224417 (2004).

53. C. T. Chantler, K. Olsen, R. A. Dragoset, J. Chang, A. R. Kishore, S. A. Kotochigova, D. S. Zucker, “X-Ray Form Factor, Attenuation and Scattering Tables” (version 2.1), (2005). [Online] Available: http://physics.nist.gov/ffast [2006, May 29]. National Institute of Standards and Technology, Gaithersburg, MD. Originally published as C. T. Chantler, J. Phys. Chem. Ref. Data **29**, 597-1048 (2000); and C. T. Chantler, J. Phys. Chem. Ref. Data **24**, 71-643 (1995).

54. E. Shiles, T. Sasaki, M. Inokuti, D. Y. Smith, “Self-consistency and sum-rule tests in the Kramers-Kronig analysis of optical data: applications to aluminium”, Phys. Rev. B **22**, 1612-1628 (1980).

55. Downloaded from the following web of Physical Reference Data, Physics Laboratory at NIST: http://physics.nist.gov/PhysRefData/FFast/Text/cover.html.

56. M. Altarelli, D. Y. Smith, “Superconvergence and sum rules for the optical constants: Physical meaning, comparison with experiment, and generalization”, Phys. Rev. B **9**, 1290–1298 (1974).

Figure captions

Fig. 1. (color online) The transmittance of Ho films with various thicknesses(in nm) normalized to the transmittance of the substrate versus the logarithm of photon energy.

Fig. 2. (Color online) Logarithm of transmittance as a function of the film thickness at five different energies (symbols) and their fit with an exponential function (lines).

Fig. 3. (color online) Log-log plot of the extinction coefficient of Ho as a function of photon energy, along with the data of Gribovskii[16] and the data of Henke *et al*.[49]

Fig. 4. (color online) The extinction coefficient of Ho as a function of photon energy at the small energy range, along with the data of Henke et al.[49]

Fig. 5. (color online) The extinction coefficient of Ho versus photon energy at the $N_{4,5}$ edge, along with data of Gribovskii et al.[16], and Henke et al.[49]

Fig. 6. (color online) The extinction coefficient of Ho versus photon energy at the $M_{4,5}$ edge: the data of Vicentin et al.[17], Ott et al.[18], Henke *et al.*[49], along with rescaled data of Vicentin et al.

Fig. 7. (color online) Log-log plot of *k* data that map a wide spectral range using the current data along with the data of Krizek[30], Vicentin et al. (after rescaling)[17], Henke *et al.*[49], and Chantler *et al.*[53], and extrapolations in the two extremes.

Fig. 8. (color online) Log-log plot of δ=1-*n* versus photon energy. The data of Henke *et al.*[49] are also represented

Fig. 9. (color online) *n* versus photon energy at the low energy range. The data of Henke et al.[49] are also represented

Fig. 10. (color online) δ=1-*n* versus photon energy at the $N_{4,5}$ edge. Henke data[49] are also represented.

Fig. 11. (color online) δ=1-*n* versus photon energy at the $M_{4,5}$ edge. . The data of Ott[18] and Henke[49] are also represented.

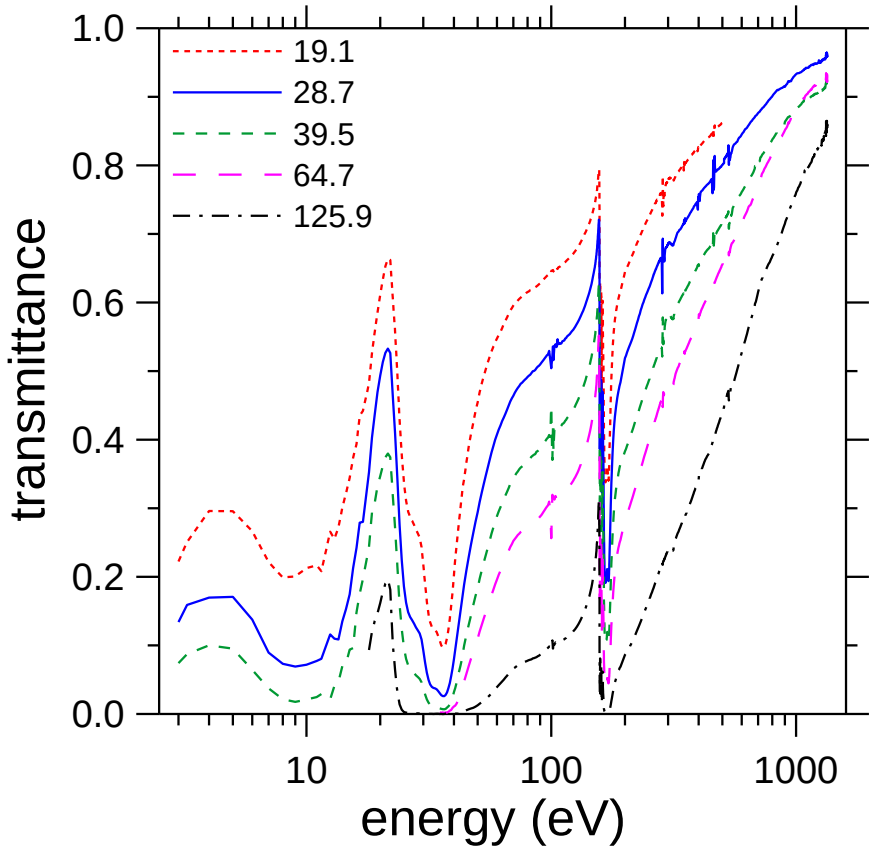
1.0
0.8
0.6
0.4
0.2
0.0
transmittance
19.1
28.7
39.5
64.7
125.9
10
100
1000
energy (eV)

Fig. 1

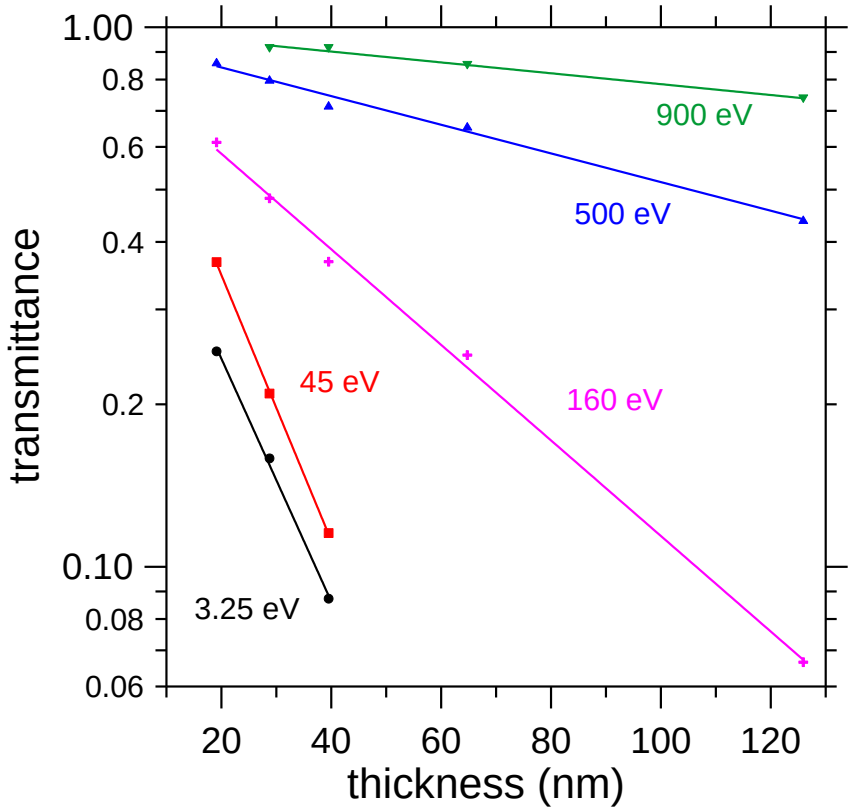
1.00
0.8
0.6
0.4
0.2
0.10
0.08
0.06
transmittance
20
40
60
80
100
120
thickness (nm)
900 eV
500 eV
160 eV
45 eV
3.25 eV

Fig. 2

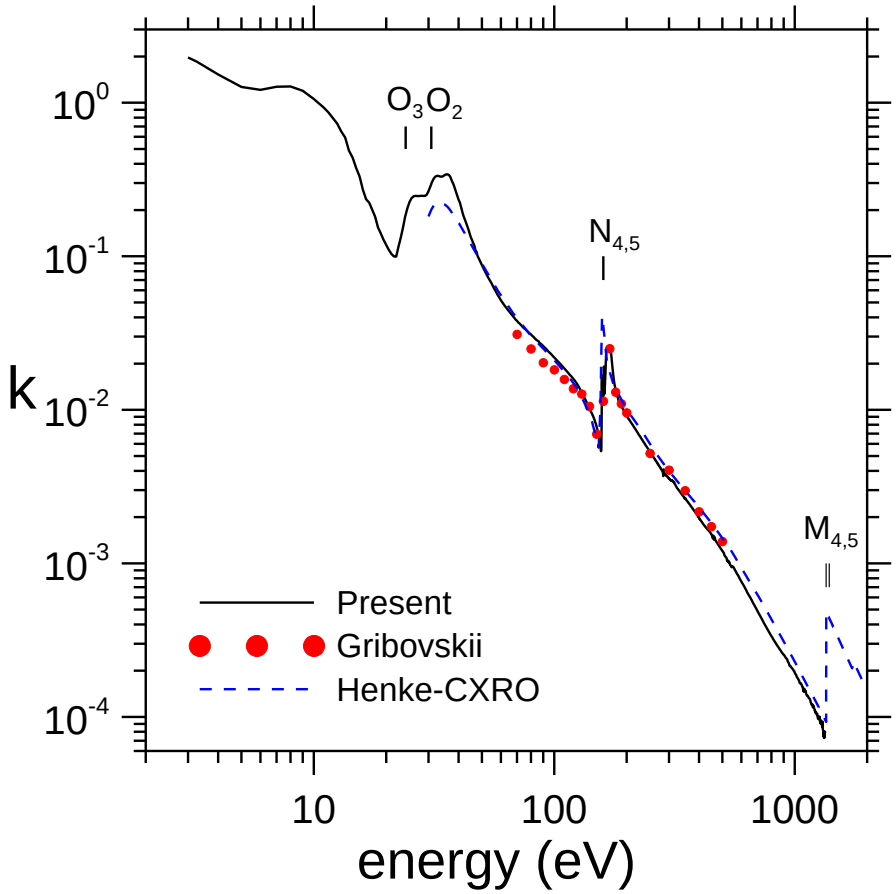
k
10^0
10^{-1}
10^{-2}
10^{-3}
10^{-4}
O_3O_2
$N_{4,5}$
$M_{4,5}$
Present
Gribovskii
Henke-CXRO
10
100
1000
energy (eV)

Fig. 3

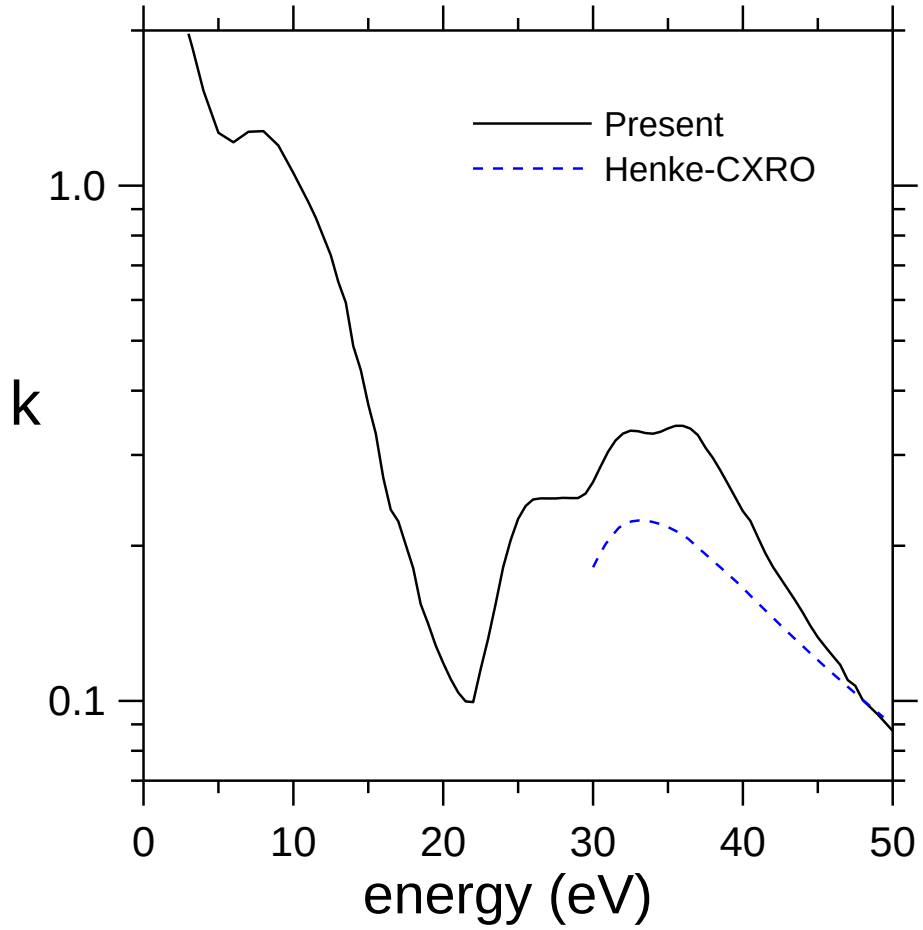

Fig. 4

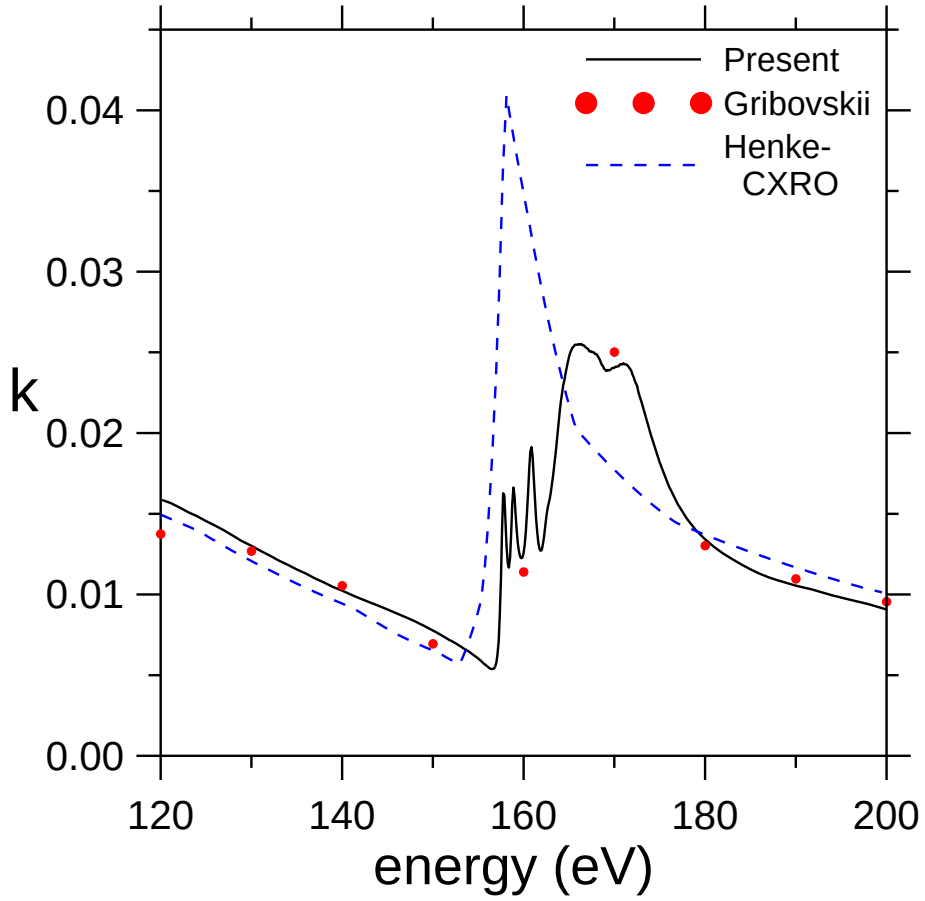
Present
Gribovskii
Henke-
CXRO
k
0.04
0.03
0.02
0.01
0.00
120
140
160
180
200
energy (eV)

Fig. 5

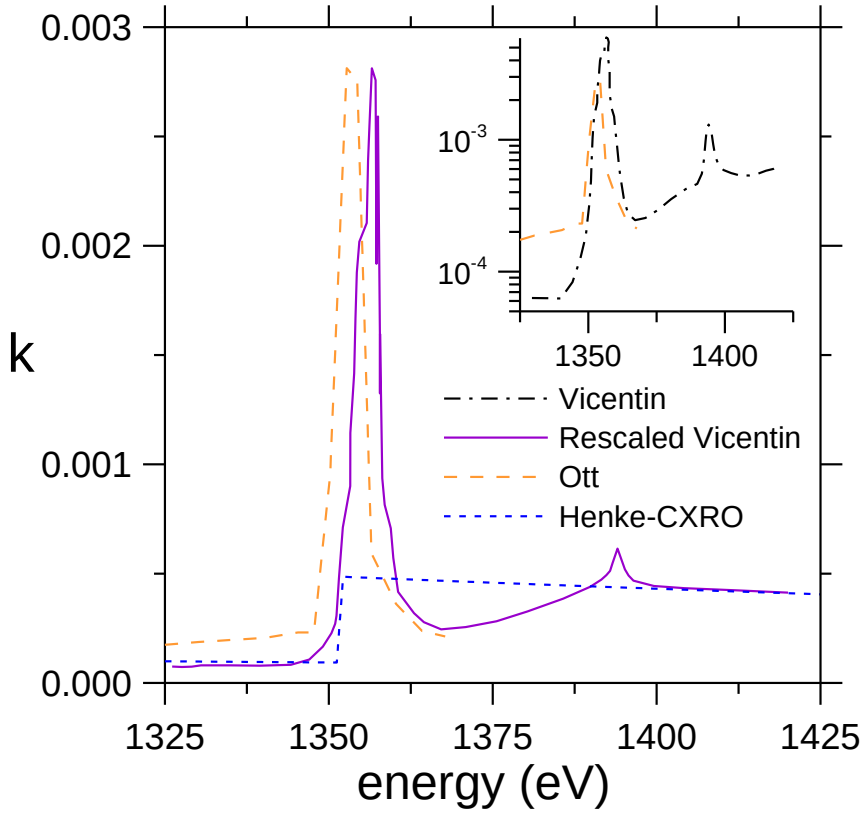
0.003
0.002
0.001
0.000
k
1325
1350
1375
1400
1425
energy (eV)
10^{-3}
10^{-4}
1350
1400
Vicentin
Rescaled Vicentin
Ott
Henke-CXRO

Fig. 6

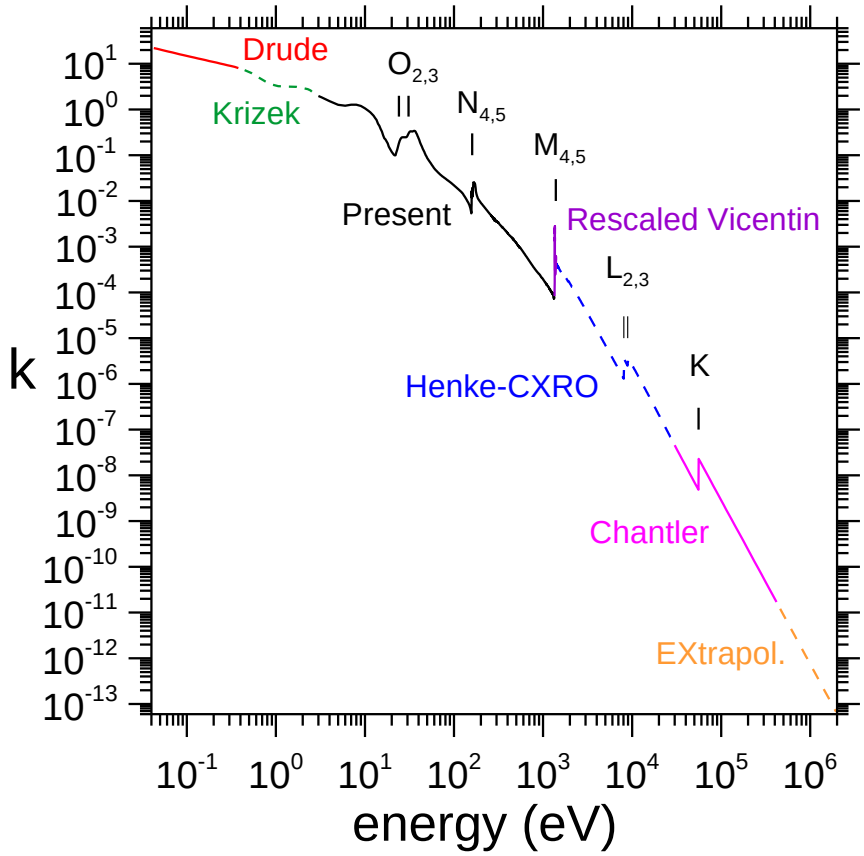
Drude
Krizek
O2,3
N4,5
M4,5
Present
Rescaled Vicentin
L2,3
K
Henke-CXRO
Chantler
EXtrapol.
k
energy (eV)

Fig. 7

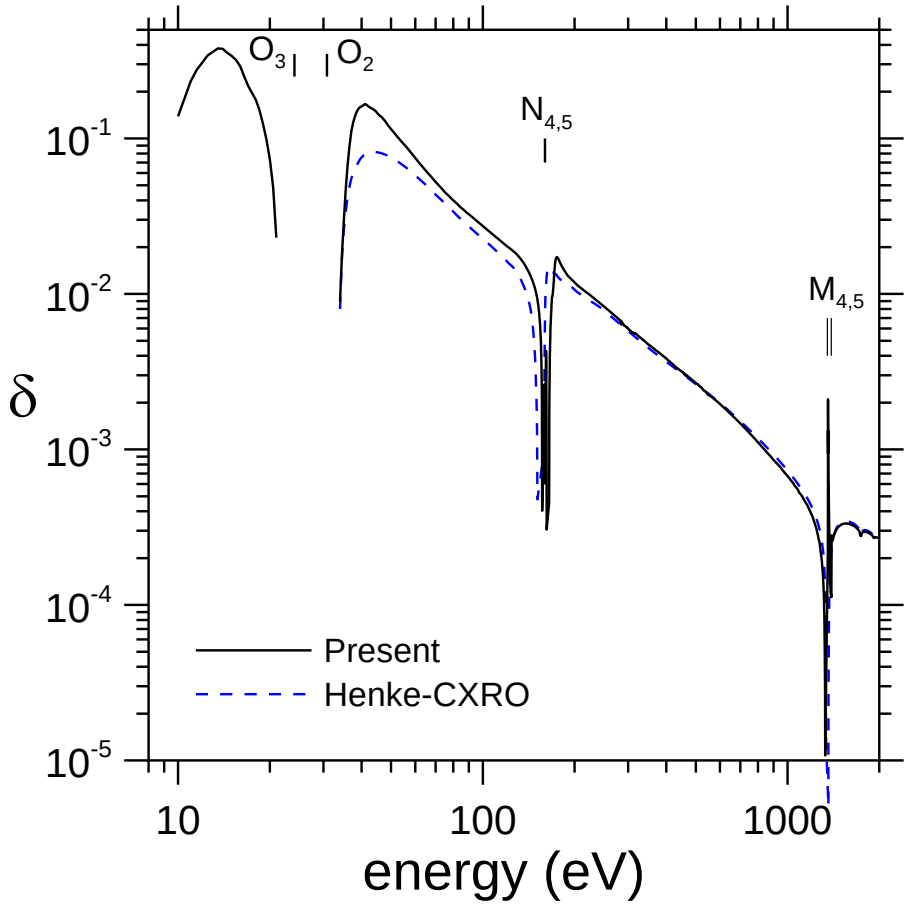
O3
O2
N4,5
M4,5
δ
10-1
10-2
10-3
10-4
10-5
10
100
1000
energy (eV)
Present
Henke-CXRO

Fig. 8

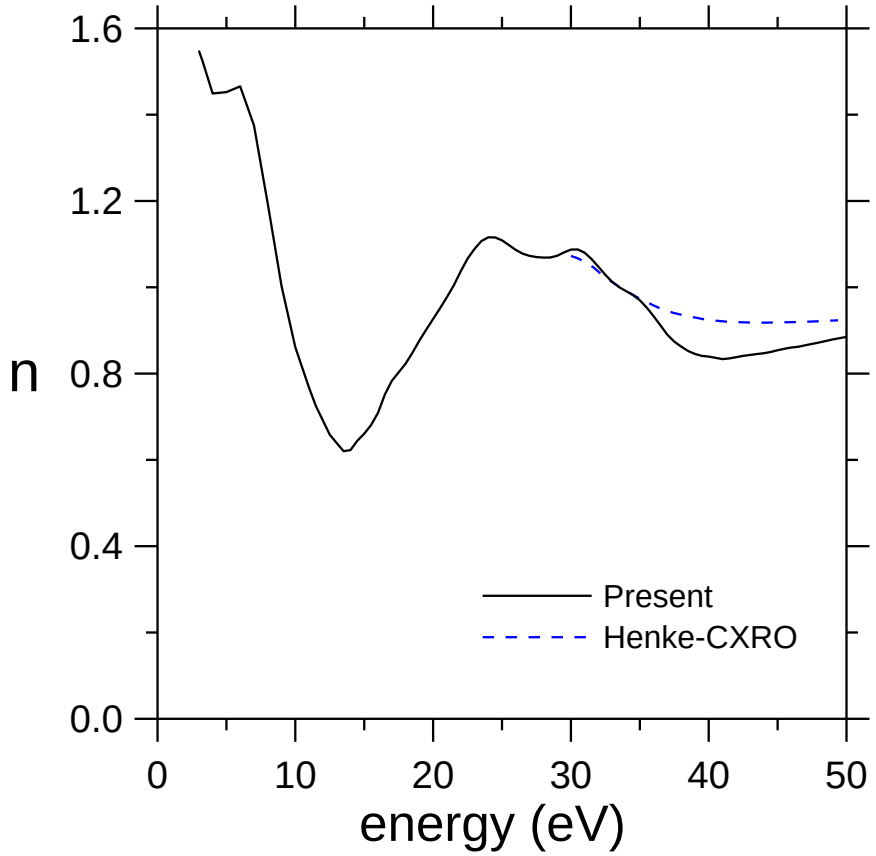

Fig. 9

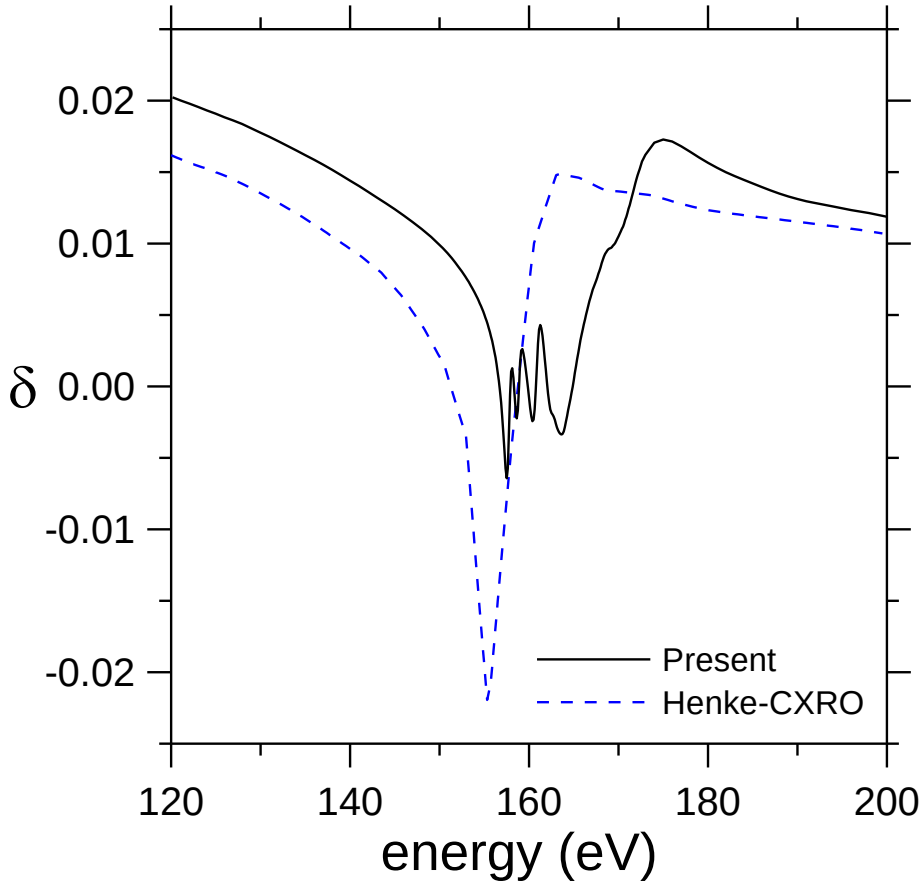
0.02
0.01
0.00
-0.01
-0.02
δ
120
140
160
180
200
energy (eV)
Present
Henke-CXRO

Fig. 10

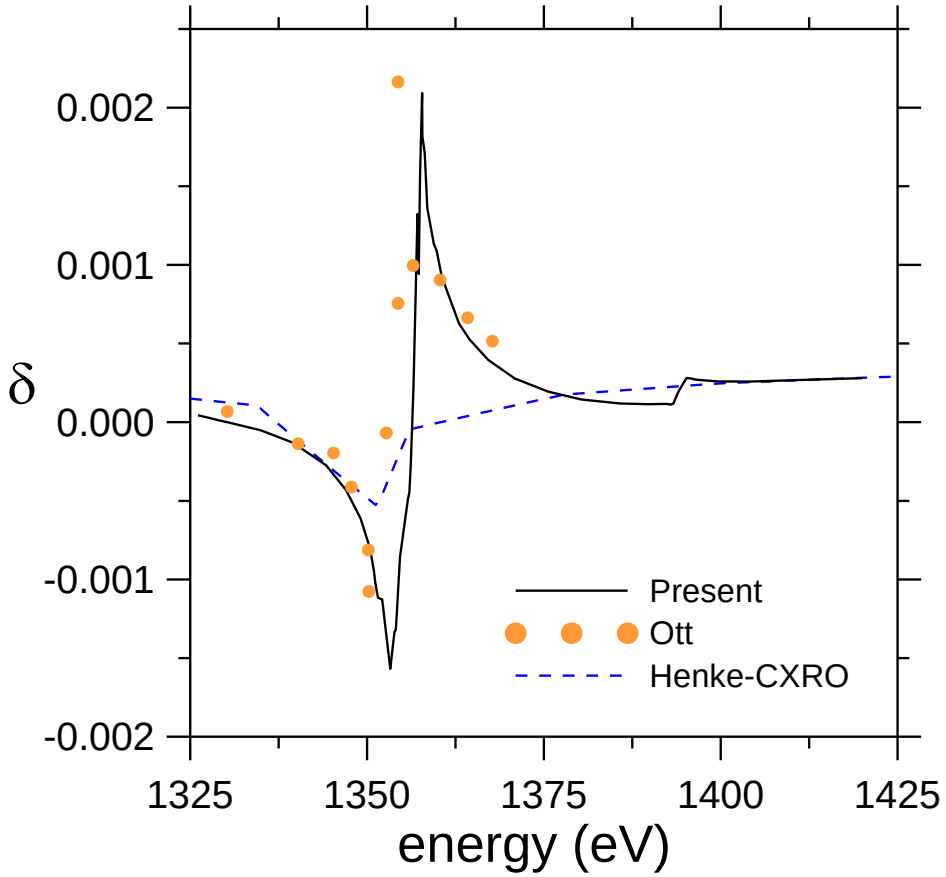
0.002
0.001
0.000
-0.001
-0.002
δ
1325
1350
1375
1400
1425
energy (eV)
Present
Ott
Henke-CXRO

Fig 11